

# Delivery of Therapeutic Doses of Radioiodine Using Bispecific Antibody-Targeted Bivalent Haptens

Emmanuel Gautherot, Jean-Marc Le Doussal, Jamila Bouhou, Corine Manetti, Marie Martin, Eric Rouvier and Jacques Barbet  
*Immunotech SA, Marseille and Hopital Pitie-Salpetriere, Laboratoire d'Immunologie Cellulaire, Paris, France*

Two-step pretargeting strategies have been designed to deliver radioisotopes to tumors more selectively than directly labeled antibodies or fragments. In this article, we compare quantitatively the potential of these strategies for the radioimmunotherapy of solid tumors. **Methods:** Direct targeting was performed using iodine-labeled IgG and  $F(ab')_2$ . As two-step strategies, we used the sequential injection of anti-CEA  $\times$  anti-DTPA-In bispecific  $F(ab')_2$  ( $BsF(ab')_2$ ) and monovalent and bivalent DTPA derivatives labeled with iodine. The biodistribution of iodine in nude mice grafted with the LS174T human colorectal carcinoma was monitored in time and used for calculating radiation doses. **Results:** In agreement with earlier studies, the IgG was more effective for delivering a radiation dose to the tumor than the  $F(ab')_2$  (7.8 versus 0.76 Gy/MBq, respectively) and both were moderately selective with respect to normal tissues (tumor:blood of 2.9 and 1.7, respectively). At their MTD, they should deliver 86 and 34 Gy, respectively, to the tumor. Using a nM-affinity DTPA-In bivalent hapten, the two-step protocol was optimized by varying the dosage of the  $BsF(ab')_2$ , the stoichiometry of the reagents and the pretargeting time. The saturation of the tumor was obtained by injecting 5 nmol (500  $\mu$ g) of  $BsF(ab')_2$ . The pretargeted  $BsF(ab')_2$  was saturated by the injection of 0.5 mol of bivalent hapten per mole of antibody. With a 48-hr pretargeting time, the selectivity of the irradiation of the tumor was optimized (tumor:blood of 7.8) but only at the price of a lower efficiency (0.35 versus 0.86 Gy/MBq, 48-hr and 20-hr pretargeting time, respectively). Attempts to increase selectivity by using a  $\mu$ M-affinity DTPA-Y bivalent hapten or by chasing excess circulating radiolabeled hapten with an excess of unlabeled hapten also reduced tumor exposure. The use of a monovalent hapten resulted in both lower efficiency and selectivity. However, the two-step pretargeting of high-affinity bivalent hapten (Affinity Enhancement System, AES) should deliver 30–60 Gy to the tumor with less than 9 Gy to the blood in tumor-bearing mice. **Conclusion:** Radioimmunotherapy with AES is predicted to be as efficient and with lower hematological toxicity than direct targeting.

**Key Words:** bispecific antibody; pretargeting; dosimetry; carcinoembryonic antigen; colon carcinoma; radioimmunotherapy

**J Nucl Med 1998; 39:1937–1943**

**R**adioimmunotherapy (RAIT) with  $^{131}$ I-labeled monoclonal antibodies has yielded contrasting clinical results, depending on the target tumor. In the treatment of refractory B cell lymphomas, complete cures have been achieved (1,2). Only partial responses have been reported so far in solid tumors because of poorer accessibility and lower radiosensitivity (3,4). One of the main limitations of the RAIT of solid tumors is the secondary toxicity, especially to the hematopoietic system.

The targeting of small radiolabeled haptens (or biotin) to pretargeted bispecific antibody (or avidin-antibody conjugates) has been designed to improve tumor-to-normal tissue ratios (5). We have developed an improved pretargeting strategy, the Affinity Enhancement System (AES), where the hapten is bivalent, thus exhibiting higher avidity for cell-bound than for

free-circulating bispecific antibody ( $BsF(ab')_2$ ). AES reagents have been demonstrated to target iodine or indium more selectively to different experimental tumors (6–8). A similar improvement was shown in clinical trials of immunoscintigraphy of CEA-expressing tumors (9). Furthermore, a preliminary clinical dosimetry study showed that  $^{131}$ I-labeled AES reagents delivered radiation doses to tumors in the range of those obtained using direct targeting (10).

Pretargeted radioimmunotherapy requires a careful optimization of the experimental protocols to achieve high and stable tumor localization combined with low normal tissue exposure. In the experiments reported here, we studied the respective influence of reagent doses, pretargeting time, valence and affinity of DTPA haptens for an anti-CEA  $\times$  anti-DTPA  $BsF(ab')_2$  on the AES pretargeting efficiency in nude mice grafted with LS174T human colorectal carcinoma. Optimized protocols with AES reagents were compared with direct targeting using IgG or  $F(ab')_2$ , in terms of dose delivery and selectivity.

## MATERIALS AND METHODS

### Human Colon Carcinoma Model in Nude Mice

The human colon carcinoma LS174T cell line was obtained from the Cell Distribution Center, American Type Culture Collection (Rockville, MD). Cells were grown in Dulbecco's modified Eagle's medium supplemented with 10% fetal bovine serum, 100 U/ml penicillin and 100  $\mu$ g/ml streptomycin (Sigma, St. Louis, MO). Cells were harvested after incubation for 5 min with trypsin-EDTA (0.05%–0.02%) at 37°C. Exponentially growing tumor cells ( $2.5 \times 10^6$ ) were grafted into 10–12 wk-old female NMRI nude mice (CERJ Le Genest, Saint Isle, France) by subcutaneous injection in the flank. Ten days later mice bearing tumors ranging from 20–200 mm<sup>3</sup> were selected for the experiments.

### Monoclonal Antibodies, Fragments and Bispecific Antibody

Anti-CEA clone F6 and anti-DTPA-metal clone 734 are mouse IgG<sub>1</sub> from Immunotech (Marseille, France). Both antibodies were purified from ascites fluid by affinity chromatography on protein A-Sepharose (Pharmacia, Uppsala, Sweden).  $F(ab')_2$  fragments were prepared by pepsin (Sigma) digestion (5% weight/weight, 2 hr at 37°C). The anti-CEA  $\times$  anti-DTPA-metal bispecific antibody ( $BsF(ab')_2$ ) was prepared by the chemical coupling of the two reduced Fab' fragments using *o*-phenylenedimaleimide according to the procedure described by Glennie et al. (11).

### Bivalent Hapten Synthesis

The monovalent DTPA hapten N- $\alpha$ -acetyl-N- $\epsilon$ -diethylenetriaminepentaacetic acid-lysyl-D-tyrosyl-N- $\epsilon$ -(glycyl-succinyl-histamine)-lysineamide (AG5.0) was synthesized, using solid-phase peptide synthesis, by Gruaz-Guyon (12).

The bivalent DTPA hapten N- $\alpha$ -diethylenetriaminepentaacetic acid-tyrosyl-N- $\epsilon$ -diethylenetriaminepentaacetic acid-lysine was prepared by reacting DTPA dianhydride with tyrosyl-lysine diac-

Received Oct. 14, 1997; revision accepted Feb. 23, 1998.

For correspondence or reprints contact: Emmanuel Gautherot, PhD, Immunotech SA, 130 avenue De Lattre de Tassigny BP 177 13276 Marseille Cedex 9, France.

etate and purified by size exclusion chromatography and reverse phase chromatography (7).

### Clearing Agent

Human serum albumin substituted with an average of 35 mol galactose and 5 mol DTPA per mole (DTPA-HSA) was obtained from Nihon Medi-Physics (Tokyo, Japan).

### Labeling

Antibodies (0.5 nmol IgG, F(ab')<sub>2</sub> or BsF(ab')<sub>2</sub>) were labeled with 18.5 MBq <sup>125</sup>I (3.7 GBq/ml; Amersham, Les Ullis, France) or <sup>131</sup>I (14.8 GBq/ml; CIS bio International, Gif sur Yvette, France) using Iodo-Gen (Pierce, Rockford, IL). The reaction was stopped by the addition of 10 nmol D,L-tyrosine (Sigma) and labeled antibodies were separated from free iodine by gel filtration on a PD-10 column (Pharmacia).

The bivalent hapten was labeled with <sup>111</sup>In using 18.5 MBq <sup>111</sup>InCl<sub>3</sub> (370 MBq/ml; Mallinckrodt, Petten, The Netherlands) for 1 nmol of hapten as already described (9). The bivalent hapten then was saturated by the addition of an excess of InCl<sub>3</sub>.

For labeling with iodide, the monovalent hapten and the bivalent hapten were dissolved at 40 μM in 0.1 M acetate, 10 mM citrate, pH 5.5 and saturated with a 25-fold excess of the metal ion. The monovalent hapten was saturated with InCl<sub>3</sub> (referred to as mono-DTPA-In), whereas the bivalent hapten was saturated either with InCl<sub>3</sub> or with YCl<sub>3</sub> (referred to as di-DTPA-In and di-DTPA-Y, respectively). Di-DTPA-In, di-DTPA-Y and mono-DTPA-In hapten were then labeled by the chloramine T (Merck, Darmstadt, Germany) method, using 37 MBq sodium [<sup>125</sup>I]iodide for 2 nmol of hapten. The labeled and unlabeled hapten were separated from free iodine by gel filtration on a PD-10 column. The specific activity was 6.7 MBq/nmol, 6.8 MBq/nmol and 8.0 MBq/nmol for di-DTPA-In, di-DTPA-Y and mono-DTPA-In, respectively.

DTPA-GSA was labeled using 18.5 MBq <sup>111</sup>InCl<sub>3</sub> for 0.1 nmol of protein. After saturation with excess InCl<sub>3</sub>, the labeled protein was purified by gel filtration on a PD-10 column.

### Reagent Purity, Reactivity and Affinity

The purity of IgG, F(ab')<sub>2</sub> and BsF(ab')<sub>2</sub> was assessed by gel filtration on a Superdex 200 column (Pharmacia). The purity of haptens was assessed by reverse-phase HPLC chromatography. Reagent purity was greater than 90%.

The immunoreactivity of the F6 moieties, as measured in anti-F6-idiotype IgG-coated tubes (which correlates with the anti-CEA immunoreactivity), and the immunoreactivity of the 734 moiety was measured on BSA-DTPA-indium-coated tubes by incubation for 15 hr at 4°C with shaking. The anti-F6-idiotype immunoreactivities were 86%, 96% and 87% for IgG, F(ab')<sub>2</sub> and BsF(ab')<sub>2</sub>, respectively. The anti-DTPA-indium immunoreactivity of the BsF(ab')<sub>2</sub> was 70%. The immunoreactivity of the labeled haptens was measured on 734 IgG coated tubes by incubation for 1 hr at 20°C with shaking. Immunoreactivity was greater than 90%. Immunoreactivity of <sup>111</sup>In-DTPA-GSA measured on 734 IgG coated tubes was 92%.

### Biodistribution Kinetics

Mice bearing LS174T tumors were injected intravenously in the tail vein with 50 μl (3.7 × 10<sup>4</sup> Bq) of radiolabeled hapten or antibody supplemented with the relevant amount of unlabeled material. At selected time intervals, animals were weighed, killed with ether and dissected. The radioactivity of major organs, tumor, blood and plasma were determined. Data on relative organ weights in mice were taken from Covell et al. (13). The results are expressed as percent of injected dose/gram of tissue (%ID/g) or percent of injected dose/milliliter (%ID/ml).

### Three-Step Experiment

The experiment was designed as follows: mice were injected with 0.2 nmol <sup>131</sup>I-labeled BsF(ab')<sub>2</sub>, 20 hr later with 0.2 nmol <sup>111</sup>In-labeled DTPA-GSA and 4 hr later, with 0.1 nmol <sup>125</sup>I-labeled di-DTPA-In. Distribution of the radioactivity in the respective organs was determined 3 hr later.

### Pharmacokinetic Analysis

The data from the biodistribution kinetics of the blood and of the tumor (% ID/g or % ID/ml) were fitted by least square regression to a sum of exponential  $a_{\alpha} \times 2^{(-t/1/2\alpha)} + a_{\beta} \times 2^{(-t/1/2\beta)} + a_{\gamma} \times 2^{(-t/1/2\gamma)}$ ,  $a_{\alpha}$ ,  $a_{\beta}$  or  $a_{\gamma}$  being either positive, when the blood clearance or release from the tumor were considered, or negative in the case of uptake by the tumor. For the blood, the sum of the pre-exponential coefficients was set equal to the % ID/ml at zero time calculated from the average mouse blood volume in the experiment, whereas for the tumor, the sum of the pre-exponential coefficients was set equal to 0.

The distribution volume (ml) was calculated as  $1/(a_{\beta} + a_{\gamma})$ . The area under the time-activity curve (AUC), expressed as % ID/g × h or % ID/ml × h, was calculated by integrating the fitted exponentials from 0 to infinite time, unless otherwise indicated. Values in the text ( $t_{1/2\alpha}$ ,  $t_{1/2\beta}$ ,  $t_{1/2\gamma}$ ,  $a_{\alpha}$ ,  $a_{\beta}$ ,  $a_{\gamma}$  or AUC) are given as the mean ± s.d.

### Dosimetry

The activity in tumor, blood and other tissues was calculated for an injection of 100% <sup>131</sup>I-labeled material by extrapolation from the measured % ID/ml or % ID/g. AUC (Bq × s/g) were calculated by integrating the fitted exponentials out to infinite time after correction for the radioactive decay of the isotope. Tissue-absorbed beta-radiation was then calculated according to Johns et al. (14) using the following formula:  $D\beta$  (Gy) =  $[1.602 \times 10^{-16} \text{ Gy} \times \text{g/Bq} \times \text{s}] \times E\beta \times \text{AUC}$  (Bq × s/g), with  $E\beta = 0.19 \text{ MeV}$ .

## RESULTS

### Biodistribution of IgG and F(ab')<sub>2</sub>

Mice grafted with LS174T colon carcinoma tumors were injected in duplicate with an isotopic dilution (3.7 × 10<sup>4</sup> Bq) of <sup>125</sup>I-labeled anti-CEA IgG or F(ab')<sub>2</sub> (0.2 nmol and 1.2 nmol total protein dose, respectively). Biodistribution was determined at nine time points from 5 min to 8 days.

The IgG distributed in a small volume (5.4 ml) and cleared very slowly from the blood (Table 1 and Fig. 1). The localization of the IgG into the tumor was slow but stable ( $t_{1/2\beta} > 200$  hr, Table 2 and Fig. 1) with a maximal value of 32.9% ± 16.1% ID/g at 48 hr. As a result, the tumor:blood AUC ratio, calculated over 192 hr (AUC<sub>0-192 hr</sub>), was moderate (Table 2). The F(ab')<sub>2</sub> distributed in a similar volume (5.2 ml) but cleared more rapidly (Table 1 and Fig. 1). The localization of the F(ab')<sub>2</sub> in the tumor was more rapid and less stable (Table 2 and Fig. 1) with a peak value at 6 hr (13.2% ± 2.4% ID/g). The tumor:blood AUC<sub>0-192 hr</sub> ratio was similar to IgG (Table 2). Similar results were obtained at a lower protein dose (0.2 nmol, not shown).

### Optimization of Use of AES Reagents

#### Biodistribution of the BsF(ab')<sub>2</sub>

Mice were injected with 0.2 nmol anti-CEA × anti-DTPA-In BsF(ab')<sub>2</sub>, and biodistribution was determined at seven time points (from 1-48 hr). The BsF(ab')<sub>2</sub> pharmacokinetic in the blood was similar to that of F(ab')<sub>2</sub>. The localization of the BsF(ab')<sub>2</sub> into the tumor was slower and less stable than that of F(ab')<sub>2</sub> but reached a higher maximum value (of 25.1% ± 0.4% ID/g after 10 hr). This is in good agreement with previously published data on modified F(ab')<sub>2</sub> fragments (15) and with the monovalent binding of the BsF(ab')<sub>2</sub> to the antigen. The

**TABLE 1**  
Pharmacokinetic Analysis from Blood Biodistribution Data\*

Antibody (nmol)	None	BsF(ab') <sub>2</sub> 1	BsF(ab') <sub>2</sub> 1	BsF(ab') <sub>2</sub> 1	F(ab') <sub>1,2</sub> 1,2	IgG 0.3
Delay (hr)	None	20	20	20	None	None
Hapten metal (nmol)	Bivalent indium 0.15	Bivalent indium 0.5	Bivalent yttrium 0.5	Monovalent indium 0.5	None	None
a $\alpha$ (% ID/ml)	41.8 $\pm$ 1.6 <sup>†</sup>	35.7 $\pm$ 0.7	38.4 $\pm$ 1.5	38.8 $\pm$ 1.0	28.2 $\pm$ 3.9	27.8 $\pm$ 0.4
t <sub>1/2</sub> $\alpha$ (min)	1.5 $\pm$ 0.3	<1 <sup>‡</sup>	<1	<1	154 $\pm$ 31	153 $\pm$ 0.5
a $\beta$ (% ID/ml)	3.1 $\pm$ 1.7	6.5 $\pm$ 1.0	8.1 $\pm$ 1.5	8.5 $\pm$ 1.0	16.8 $\pm$ 3.8	18.6 $\pm$ 0.4
t <sub>1/2</sub> $\beta$ (hr)	0.3 $\pm$ 0.1	11.8 $\pm$ 3.2	0.5 $\pm$ 0.1	4.2 $\pm$ 0.7	11.9 $\pm$ 1.7	163.0 $\pm$ 2.8
a $\gamma$ (% ID/ml)	0.07 $\pm$ 0.05	0.3 $\pm$ 0.9	0.04 $\pm$ 0.02	0.05 $\pm$ 0.05	0.08 $\pm$ 0.13	—
t <sub>1/2</sub> $\gamma$ (hr)	8.2 $\pm$ 5.9	31.5 $\pm$ 24.7	37.5 $\pm$ 16.7	44.8 $\pm$ 31.1	>200	—
AUC (% ID/ml $\times$ hr)	3.7 $\pm$ 0.5 <sup>§</sup>	125 $\pm$ 15 <sup>§</sup>	8.9 $\pm$ 1.0 <sup>§</sup>	55 $\pm$ 7 <sup>§</sup>	403 $\pm$ 14 <sup>¶</sup>	2547 $\pm$ 51 <sup>¶</sup>

\*Data fitted on a 0 to 8 days time scale except for the bivalent hapten alone (0 to 24 hr).

<sup>†</sup>Mean  $\pm$  s.d.

<sup>‡</sup>Half-life smaller than the first experimental time.

<sup>§</sup>AUC<sub>0- $\infty$</sub>

<sup>¶</sup>AUC<sub>0-192 hr</sub>

tumor:blood uptake ratio was 1.1  $\pm$  0.4, 3.6  $\pm$  0.7, and 11.1  $\pm$  0.5 at 6, 20 and 48 hr, respectively.

#### Determination of Saturating BsF(ab')<sub>2</sub> Injected Dose

Mice were injected with increasing amounts of <sup>125</sup>I-labeled BsF(ab')<sub>2</sub>, and biodistribution was determined 24 hr after injection (Fig. 2). The accumulation of BsF(ab')<sub>2</sub> in the tumor tended to saturate when the injected dose exceeded 5 nmol. In parallel, the tumor:blood uptake ratio decreased.

#### Biodistribution of Free Bivalent Hapten

After the administration of 150 pmol of <sup>125</sup>I-labeled di-DTPA-In to tumor bearing mice, the radioactivity distributed rapidly in a large volume (31.1 ml) and cleared with a t<sub>1/2</sub> $\beta$  of 0.3  $\pm$  0.1 hr (Table 1). A very small fraction circulated longer but did not correspond to any significant blood activity after 24 hr (<0.01% ID/ml). Biodistribution at 6 hr showed very low residual activities (<0.2% ID/g) in the tumor and in all tissues examined, with the exception of the kidneys (0.8%  $\pm$  0.1% ID/g). As expected, the free hapten perfused the tumor very transiently (half-lives in minutes, Table 2).

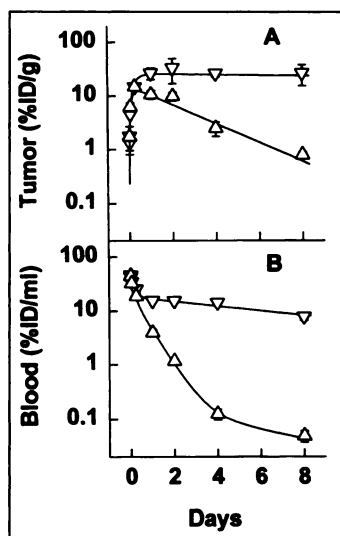


**FIGURE 1.** (A) Biodistribution kinetics in tumor and (B) in blood of 0.2 nmol <sup>125</sup>I-labeled F6 IgG ( $\nabla$ ) and 1.2 nmol <sup>125</sup>I-labeled F6 F(ab')<sub>2</sub> ( $\Delta$ ). Mean  $\pm$  s.d. Solid lines represent curves corresponding to parameters reported in Tables 1 and 2.

#### Saturation of Pretargeted BsF(ab')<sub>2</sub> by Increasing Doses of Bivalent Hapten

Mice were injected with a constant amount of <sup>125</sup>I-labeled BsF(ab')<sub>2</sub> and, 24 hr later, with increasing amounts of <sup>111</sup>In-bivalent hapten (Fig. 3). Under all the experimental conditions tested (see the figure legend), the amount of bivalent hapten that localized in the tumor tended to meet a plateau (Fig. 3A). This plateau was found to correspond reasonably well, especially regarding the biodistribution data at 48 hr, to the quantity of pretargeted BsF(ab')<sub>2</sub>, in terms of bivalent binding sites, calculated taking into account the BsF(ab')<sub>2</sub> uptake by the tumor and its anti-DTPA-In immunoreactivity (1.9  $\pm$  0.8, 1.3  $\pm$  0.3 and 0.7  $\pm$  0.2 pmol/g at 6, 24 and 48 hr, respectively). This suggests that, in the tumor, the bivalent hapten preferentially cross-links two BsF(ab')<sub>2</sub> molecules.

Conversely, the amount of bivalent hapten localized in the kidneys (Fig. 3B) increased linearly with the dose of bivalent hapten, a property typical of nonspecific uptake. Moreover, the amount of bivalent hapten exceeded the quantity of pretargeted BsF(ab')<sub>2</sub>, in terms of DTPA binding sites (0.10  $\pm$  0.02, 0.05  $\pm$  0.01 and 0.02  $\pm$  0.004 pmol/g at 6, 24 and 48 hr, respectively).

In the blood, the concentration of bivalent hapten (Fig. 3C) was independent of the hapten injected dose at 24 and 48 hr, but not at 6 hr. Furthermore, this concentration was significantly lower than the concentration of anti-DTPA BsF(ab')<sub>2</sub> binding sites under all the experimental conditions tested (0.35  $\pm$  0.09, 0.16  $\pm$  0.03 and 0.04  $\pm$  0.02 pmol/g at 6, 24 and 48 hr, respectively), suggesting that the bivalent hapten did not saturate the circulating BsF(ab')<sub>2</sub> at the steady state.

#### Increasing Pretargeting Time

Mice were injected with 0.2 nmol BsF(ab')<sub>2</sub> and, after a variable delay (6, 20 and 48 hr), with 0.1 nmol bivalent hapten. The biodistribution was determined 24 hr later. Increasing the pretargeting time reduced the uptake of the bivalent hapten in all organs dissected. However, the uptake ratios for all organs except the kidneys increased (Fig. 4).

#### Decreasing Hapten Affinity

Di-In-DTPA has a high affinity for the anti-DTPA antibody (K<sub>a</sub> = 3.1  $\pm$  0.6 nM<sup>-1</sup>) that depends on the presence of the indium ion inside the chelate. A lower affinity hapten (K<sub>a</sub> =

**TABLE 2**  
Pharmacokinetic Analysis from Tumor Biodistribution Data\*

Antibody (nmol)	None	BsF(ab') <sub>2</sub> 1	BsF(ab') <sub>2</sub> 1	BsF(ab') <sub>2</sub> 1	F(ab') <sub>2</sub> 1.2	IgG 0.3
Delay (hr)	None	20	20	20	None	None
Hapten metal (nmol)	Bivalent indium 0.15	Bivalent indium 0.5	Bivalent yttrium 0.5	Monovalent indium 0.5	None	None
Rapid α (% ID/g)	5.7 ± 4.6 <sup>†</sup>	8.1 ± 1.1	6.9 ± 1.4	13.3 ± 3.0	—	—
Uptake t <sub>1/2α</sub> (min)	4.1 ± 2.2 <sup>‡</sup>	4.0 ± 1.0	2.1 ± 0.9	12.4 ± 5.7	—	—
Slow αβ (% ID/g)	—	11.0 ± 6.7	—	—	15.1 ± 3.3	26.0 ± 6.7
Uptake t <sub>1/2β</sub> (hr)	—	10.4 ± 8.0	—	—	2.0 ± 0.8	3.9 ± 1.7
Rapid αβ (% ID/g)	5.5 ± 4.6	—	4.7 ± 1.4	12.6 ± 3.0	—	—
Release t <sub>1/2β</sub> (hr)	0.2 ± 0.1	—	3.3 ± 2.2	11.2 ± 4.4	—	—
Slow αγ (% ID/g)	0.14 ± 0.04	19.1 ± 6.9	2.2 ± 0.7	0.7 ± 1.8	15.1 ± 3.3	26.0 ± 6.7
Release t <sub>1/2γ</sub> (hr)	9.1 ± 2.8	41.7 ± 7.3	36.6 ± 7.5	48.6 ± 52.6	41.3 ± 7.6	>200
AUC (% ID/g × hr)	2.8 ± 0.4 <sup>§</sup>	983 ± 77 <sup>§</sup>	140 ± 19 <sup>§</sup>	251 ± 43 <sup>§</sup>	821 ± 116 <sup>¶</sup>	4559 ± 3927 <sup>¶</sup>
Tumor/Blood AUC	0.75 ± 0.2	7.9 ± 1.1	15.7 ± 2.8	4.5 ± 1.0	2.0 ± 0.3	1.8 ± 1.5

\*Data fitted on a 0 to 8 days time scale except for the bivalent hapten alone (0 to 24 hr).

<sup>†</sup>The sum of the pre-exponential coefficients was set equal to 0 at 0 time. Thus, in the calculation, the sign of the pre-exponential coefficients for the uptake was negative.

<sup>‡</sup>Mean ± s.d.

<sup>§</sup>AUC<sub>0-∞</sub>

<sup>¶</sup>AUC<sub>0-192 hr</sub>

2.7 ± 0.4 μM<sup>-1</sup>) was obtained by saturating the DTPA group with yttrium. Mice were thus injected with 1 nmol BsF(ab')<sub>2</sub> and 20 hr later, with 0.5 nmol of either di-DTPA-Y, di-DTPA-In or mono-DTPA-In hapten (as a control high-affinity monovalent hapten, K<sub>a</sub> of 3.6 ± 0.8 nM<sup>-1</sup>).

In the blood (Table 1 and Fig. 5), di-DTPA-Y distributed in a similar volume as di-DTPA-In, but cleared 23 times faster, as expected from its lower affinity for the BsF(ab')<sub>2</sub>. Interestingly, the high-affinity monovalent DTPA-In cleared three times faster. Only a very small fraction (0.3%–0.04% ID/ml) cleared very slowly. The AUC<sub>0-∞</sub> for the blood was reduced about 14 and 2 times, for di-DTPA-Y and mono-DTPA-In, respectively, as compared with di-DTPA-In.

In the tumor (Table 2 and Fig. 5), the localization of di-DTPA-Y when compared with di-DTPA-In was only transient, although significant when compared to that of the free hapten. Mono-DTPA-In localization had an intermediate stability. The AUC<sub>0-∞</sub> for the tumor was reduced about seven and four times, respectively, as compared with di-DTPA-In. As a result, the tumor:blood AUC<sub>0-∞</sub> ratio was higher with di-DTPA-Y (15.7 ± 2.8) than with di-DTPA-In (7.9 ± 1.1) but lower with mono-DTPA-In (4.5 ± 1.0). Interestingly, the uptake into the tumor was monophasic for di-DTPA-Y and DTPA-In whereas it was biphasic for di-DTPA-In. We interpret the rapid phase as the direct uptake of the free hapten by

pretargeted BsF(ab')<sub>2</sub> and the second phase as the transport of circulating hapten/BsF(ab')<sub>2</sub> complexes to the tumor.

### Chase Experiments

To clear the circulating BsF(ab')<sub>2</sub> before the injection of the hapten, we used human serum albumin substituted with both DTPA and galactose (DTPA-GSA). In vitro, indium-DTPA-GSA (K<sub>a</sub> = 3 × 10<sup>7</sup> M<sup>-1</sup> for anti-DTPA-indium Fab) was able to complex the BsF(ab')<sub>2</sub> as assessed by gel filtration analysis and, in vivo, it was found to redirect circulating BsF(ab')<sub>2</sub> into the liver in a dose-dependent manner (data not shown).

In the three-step experiment, <sup>111</sup>In-labeled DTPA-GSA ac-

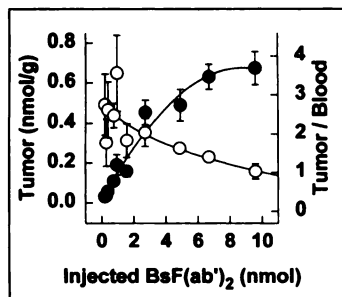


**FIGURE 2.** Tumor localization (●) and tumor:blood uptake ratio (○) 24 hr after administration of increasing amounts of <sup>125</sup>I-labeled BsF(ab')<sub>2</sub>. Mean ± s.d.

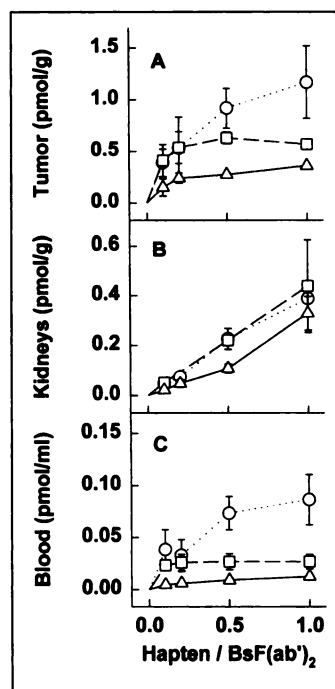
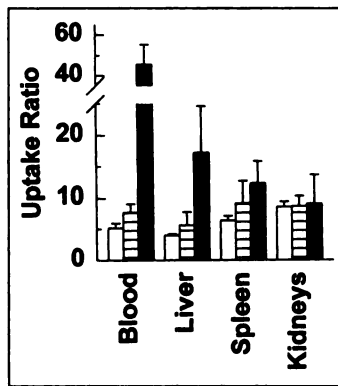


**FIGURE 3.** Localization of increasing doses of bivalent hapten to pretargeted BsF(ab')<sub>2</sub> (A) in tumor, (B) kidneys and (C) blood. Mice were injected with 26 pmol <sup>125</sup>I-labeled BsF(ab')<sub>2</sub> and 24 hr later with various amounts (2.6, 5.2, 13 and 26 pmol) of <sup>111</sup>In-labeled di-DTPA-In. Bivalent hapten localizations are shown at 6 (●), 24 (□) and 48 hr (△) posthapten injection.

**FIGURE 4.** Variation of pretargeting time. Mice were injected with 0.2 nmol BsF(ab')<sub>2</sub> and after either 6 hr (□), 24 hr (▨) or 48 hr (■) with 0.1 nmol <sup>125</sup>I-labeled di-DTPA-In. Organ distribution was determined 24 hr after bivalent hapten administration. Mean ± s.d. In tumor, localizations were 14.4 ± 1.5, 9.0 ± 2.0 and 6.1% ± 1.5% ID/g for 6-, 20- and 48-hr pretargeting time, respectively.



accumulated mainly in the liver (54.4% ± 13.2% ID/g). The concentration of the <sup>131</sup>I-labeled BsF(ab')<sub>2</sub> in the blood was twice as low as in the control (no chase, 6.0 ± 1.0 versus 3.3% ± 0.3% ID/ml). By contrast, its biodistribution in the tumor and major organs was not altered (data not shown). Thus, the bivalent hapten concentration was reduced twofold in the blood (2.9 ± 0.5 versus 1.4% ± 0.2% ID/ml) and in major organs but not in the tumor (5.4 ± 2.9 versus 9.3% ± 2.0% ID/g). As a consequence, tumor:organ uptake ratios were improved with the exception of the kidneys (Fig. 6).

The injection of an excess of free unlabeled hapten to clear circulating labeled hapten had been proposed earlier as a mechanism for enhancing selectivity in pretargeting experiments (16). Therefore, mice were injected with preformed BsF(ab')<sub>2</sub>-<sup>125</sup>I-labeled bivalent hapten complexes (0.1 and 0.05 nmol, respectively) and 16 hr later, with a 1–1000 times molar excess of unlabeled bivalent hapten (0.05–50 nmol, Fig. 7a) or monovalent hapten (data not shown). The monovalent and the bivalent haptens had very similar effects on the distribution of the labeled hapten in the blood and in the tumor. All the blood-borne activity could be chased in a dose-dependent way, up to 60% of the activity was chased from the tumor using a very large excess of unlabeled hapten. As expected, the injection of unlabeled hapten did not reverse the uptake of the labeled bivalent hapten in the kidneys and in catabolizing organs such as the liver (Fig. 7A).

As the injection of a 1000-fold excess of free hapten cleared more activity from the blood than from the tumor, the biodistribution kinetic was monitored before and after the chase (Fig. 7 B and C). Without chase, the localization of preformed BsF(ab')<sub>2</sub>-hapten complexes was slow (half-life 3.1 ± 2.5 hr) but very stable (release half-life ≈ 200 hr; Fig. 7B). The bivalent hapten distributed in a small volume (9.0 ml) and was

**FIGURE 5.** Effect of hapten affinity and valence. Mice were injected with 1 nmol BsF(ab')<sub>2</sub> and 20 hr later with either 0.5 nmol <sup>125</sup>I-labeled di-DTPA-In (—●—), di-DTPA-Y (—○—) or mono-DTPA-In hapten (—□—). Mean ± s.d. Solid lines represent curves corresponding to parameters reported in Tables 1 and 2.

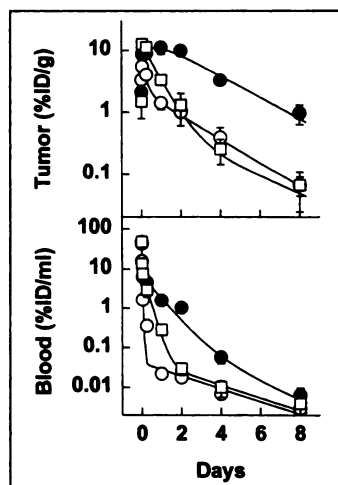
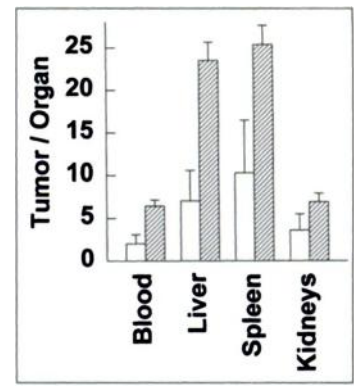


**FIGURE 6.** Tumor:organ uptake ratios after chase with DTPA-GSA. Mice were injected with 0.2 nmol <sup>131</sup>I-labeled BsF(ab')<sub>2</sub>, 20 hr later with 0.2 nmol <sup>111</sup>In-labeled DTPA-GSA and 4 hr later with 0.1 nmol <sup>125</sup>I-labeled di-DTPA-In (▨). Control experiment was performed without clearing step (□). Tumor:organ uptake ratios are shown at 3 hr. Mean ± s.d.



cleared with a t<sub>1/2β</sub> of 10.9 ± 2.8 hr (Fig. 7C). In the blood, 95% of the bivalent hapten was chased and cleared as rapidly as the free hapten (half-life = 0.25 ± 0.04 hr, and Table 1). In the tumor, the chased hapten dissociated also as rapidly as the free hapten (half-life of 0.17 ± 0.09 hr and Table 1). The remaining fraction was released slowly with a half-life of 32.0 ± 9.0 hr (Fig. 7B). This slow phase may represent either the dissociation of highly cooperative bivalent hapten-BsF(ab')<sub>2</sub> complexes or the release of sequestered (or internalized) bivalent hapten.

This chase protocol considerably improved tumor:blood uptake ratios (10 times at 6 hr after the chase) but did not improve AUC ratios. Indeed, it had a minor effect on blood AUC<sub>0–63 hr</sub> (229 vs. 290% ID/ml × hr) since the AUC in the blood was determined mainly by early time points. Conversely, it lowered the tumor AUC<sub>0–63 hr</sub> twofold (306 vs. 787% ID/g × hr).

#### Dosimetry

Dosimetry was calculated for direct targeting with IgG and F(ab')<sub>2</sub>, AES targeting with 1 nmol BsF(ab')<sub>2</sub>, 20 hr pretargeting time and 0.5 nmol of di-DTPA-In (referred to as AES 1/20/0.5) and AES targeting with 5 nmol BsF(ab')<sub>2</sub>, 48 hr pretargeting time and 2.5 nmol di-DTPA-In (referred to as AES

**FIGURE 7.** Postchase experiments. (A) Mice were injected simultaneously with 100 pmol BsF(ab')<sub>2</sub> and 50 pmol <sup>125</sup>I-labeled di-DTPA-In, and 16 hr later, with saline solution (—■—) or with a 1- (—●—), 10- (—▨—), 100- (—□—), or 1000-molar (—▨—) excess of unlabeled di-DTPA-In. Organ distribution was determined 1 hr postchase (Tu = tumor, BI = blood, Ki = kidneys). (B, C) Tumor and blood pharmacokinetics with or without a chase step. Mice were injected as in (A) and 16 hr after, with 1000-molar excess of unlabeled di-DTPA-In (—●—) or with saline solution (—○—). Mean ± s.d.

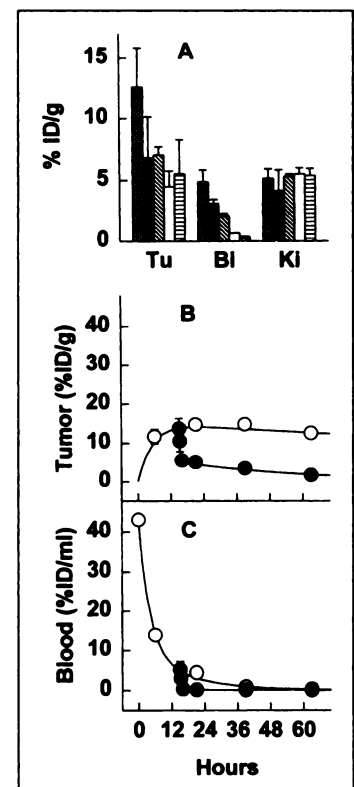


**TABLE 3**  
Tumor and Normal Tissue Absorbed Radiation Doses (Gy)\*

	AES targeting		Direct targeting	
	AES 1/20/0.5	AES 5/48/2.5	IgG	F(ab') <sub>2</sub>
Tumor	31.9 ± 16.4 <sup>†</sup>	64.1 ± 15.9	86.2 ± 22.5	33.9 ± 6.2
Blood	4.7 ± 1.9	8.2 ± 2.8	30.1 ± 4.3	17.8 ± 3.6
Tumor/Blood	6.7 ± 4.4 <sup>‡</sup>	7.8 ± 3.3	2.9 ± 0.9	1.9 ± 0.5
Tumor/Liver	10.3 ± 5.4	7.1 ± 2.2	6.8 ± 1.6	9.5 ± 2.8
Tumor/Spleen	12.1 ± 6.6	12.4 ± 5.4	4.1 ± 1.0	12.3 ± 5.1
Tumor/Kidneys	7.0 ± 3.7	4.9 ± 1.4	6.9 ± 2.6	5.9 ± 1.4

\*Estimation based on an administered activity of 37 MBq <sup>131</sup>I-labeled bivalent hapten (0.5 nmol, AES 1/20/0.5), 185 MBq <sup>131</sup>I-labeled bivalent hapten (2.5 nmol, AES 5/48/2.5), 11.1 MBq <sup>131</sup>I-labeled IgG (0.2 nmol) and 44.4 MBq <sup>131</sup>I-labeled F(ab')<sub>2</sub> (1.2 nmol).

<sup>†</sup>Absorbed radiation dose (Gy), mean ± s.d.

<sup>‡</sup>Absorbed radiation dose ratio, mean ± s.d.

5/48/2.5). For IgG and F(ab')<sub>2</sub>, the activity was calculated taking into account the protein dose used in the experiment and the maximal specific activity described in the literature for antibodies labeled with <sup>131</sup>I (370 MBq/mg). As the half-life of the release of the IgG from the tumor could not be calculated, the integration on the IgG tumor data were done based solely on the physical half-life of the isotope. The di-DTPA-In hapten can be labeled with high specific activity [up to 74 MBq/nmol (10), Gautherot, unpublished data, 1995]. Thus, calculations were made assuming <sup>131</sup>I injected activities of 11.1 MBq for IgG, 44.4 MBq for F(ab')<sub>2</sub> which corresponds to their respective MTD (17) and, 37 MBq and 185 MBq for the AES protocols. Under these conditions (Table 3), the calculated cumulated doses to the tumor and tissues by direct targeting with IgG or F(ab')<sub>2</sub> were in good agreement with those reported in the literature (18). Similarly, both AES protocols appeared capable of delivering high radiation doses to the tumor. AES 1/20/0.5 was predicted to have an efficiency close to F(ab')<sub>2</sub> and AES 5/48/2.5 was predicted to be as efficient as IgG (Table 3).

## DISCUSSION

The success of radioimmunotherapy requires high and stable tumor localization combined with low exposure of normal tissues. RAIT protocols with directly labeled antibodies are limited by the toxicity to the hematopoietic system, the bone marrow being the most radiosensitive organ. Thus, pretargeting approaches have been designed to reduce the exposure of normal tissues to radiation. However, unlike direct targeting, pretargeting strategies must be optimized carefully with respect to the doses and administration schedules (19,20).

The simulations performed by Baxter et al. (21) with a physiologically-based pharmacokinetic model suggest that the optimal dose of bispecific antibody should be just sufficient to saturate the antigen-binding sites in the tumor. Similarly, the hapten dose should be just sufficient to saturate the antibody present in the tumor, and the pretargeting time interval should be long enough to give high tumor-to-blood concentration ratios at hapten injection. In these experiments, we used the same bispecific antibody (BsF(ab')<sub>2</sub>) and, in addition to the above mentioned parameters, we examined the effect of the valence and the affinity of the hapten for the BsF(ab')<sub>2</sub> on the performance of AES pretargeting for RAIT.

In the experiments presented here, particular attention was given to the BsF(ab')<sub>2</sub> to hapten molar ratio to achieve maximal uptake of bivalent hapten by the tumor while limiting the nonspecific uptake by catabolizing tissues. Provided that the BsF(ab')<sub>2</sub> dose did not exceed 5 nmol, a molar ratio of 0.5 appeared to be the best compromise.

We (7,22) and others (23) have shown the benefit of pretargeting using low doses of bispecific antibody and bivalent hapten. Similarly, therapeutic doses of bivalent hapten exhibited significantly higher targeting efficacy (high uptake and stability) and better selectivity than equivalent doses of monovalent hapten. Although at early time points, monovalent and bivalent hapten bound similarly to the BsF(ab')<sub>2</sub> in the blood and in the tumor, the final difference results from the slower release of the bivalent hapten from the tumor. Similar instability of monovalent haptens (K<sub>a</sub> antihapten 0.1–14 nM<sup>-1</sup>) has been reported in different experimental models and with other pretargeting systems (20,24,25). Furthermore, using a μM-affinity bivalent hapten increased the selectivity for the tumor in terms of AUC ratio but at the price of a dramatic loss of targeting efficacy. This suggests that high affinity is required for targeting efficacy, but that the selectivity ultimately relies on the affinity enhancement effect and on the distribution of the BsF(ab')<sub>2</sub> at the time of hapten injection.

The selectivity of the distribution of the modified antibody itself is of major importance. Several ways have been suggested to enhance this selectivity, including the increase of the pretargeting time and the augmentation of its affinity for the target antigen. Our data, in agreement with those of other workers (20), show that longer pretargeting intervals improved the selectivity but at the expense of reduced tumor localization. In this tumor model, a 10-fold increase in affinity (10<sup>9</sup> to 10<sup>10</sup> M<sup>-1</sup>) did not affect the release half-life of F(ab')<sub>2</sub> fragments from the tumor (unpublished data) suggesting that the shedding and/or the internalization, although moderate, of the CEA (26) may become the limiting factor.

With pretargeting strategies, the complexes between the modified antibody and the radiolabeled second component that form in the blood contribute largely to the activity in the blood. It has been shown, both experimentally (16) and in the clinic (27), that the use of an additional clearing step, in which the concentration of the modified antibody is decreased before administration of the radiolabeled species, reduces this source of activity. We introduced a chase step after the administration of the labeled bivalent hapten to reverse its binding to the BsF(ab')<sub>2</sub>. This approach is of limited interest for RAIT since the AUC was reduced in the tumor and unchanged in the main organs. However, the chase protocol may be used in immunoscintigraphy since it considerably improved tumor: blood ratios at early time points. More interesting for RAIT is the elimination of the circulating BsF(ab')<sub>2</sub> before hapten injection by redirecting the antibody to the hepatic asialoglycoprotein receptor. This approach has been used successfully in the clinic

for clearing the excess of circulating antibody-streptavidin conjugate prior  $^{111}\text{In}$ -labeled DOTA-biotin administration (28). In the experiment presented here, the clearing efficiency of indium-DTPA-GSA was limited. In our view, two reasons may account for this: unlike in the above mentioned system, the concentration of  $\text{BsF}(\text{ab}')_2$  in the blood at the clearing step was already low when compared to that of the streptavidin-antibody conjugate and the affinity of indium-DTPA-GSA for the  $\text{BsF}(\text{ab}')_2$  is  $10^8$  times lower than that of biotin for avidin.

Several experimental studies in mice grafted with human colon carcinoma have shown antitumor effects with  $^{131}\text{I}$ -labeled antibodies with estimated radiation doses to the tumor ranging from 10–90 Gy (29). In this study, the experimental protocols with IgG,  $\text{F}(\text{ab}')_2$  and AES that were selected for dosimetry were predicted to deliver from 30–90 Gy to the tumor (Table 3).

For a similar cumulated dose, the AES pretargeting may be more efficient than direct targeting, especially with IgG, because of a more homogeneous radiation dose throughout the tumor depending on the rapid diffusion of the bivalent hapten to the center of the tumor (19) and on the relatively rapid diffusion of the  $\text{BsF}(\text{ab}')_2$ . Rapid uptake kinetics with the AES were observed also in several CEA-expressing multicell spheroids, using the same reagents (30).

In a recent clinical RAIT study, the dose limit to the red marrow was shown to be 4.5 Gy (4). In rodents, the dose limit is generally higher, 6–9 Gy (31). As the activity in the marrow may be considered as a fraction of the activity in the blood (32), we predict here that RAIT in the mouse model with AES pretargeting should be less toxic (Table 3). After the blood, the kidney, the liver and the spleen may be the dose limiting organs since AUC ratios were not improved with the AES compared to direct targeting, presumably because of prolonged intracellular retention of the activity (33).

The interest of AES pretargeting has been confirmed by a clinical dosimetry study in patients with medullary thyroid cancer and small-cell lung cancer (10). This study showed that AES pretargeting achieved high absorbed doses (11–470 Gy/MBq), especially in the case of small-sized MTC recurrences. It has been proposed that the dose scale-up from mouse to human should not be calculated from body mass ratios ( $\approx 2500$  times) but rather as the  $3/4$  power of this ratio (34) ( $\approx 350$  times). Thus, the 37 MBq injected to mice would correspond to 13 GBq in humans, which is an acceptable activity in terms of the medical care safety requirements. In parallel, the dose of bispecific antibody would be increased to 100–200 mg.

## CONCLUSION

AES pretargeting RAIT protocols could be designed to deliver higher radiation doses to the tumor with comparable hematological toxicity as direct targeting using labeled IgG or  $\text{F}(\text{ab}')_2$ . Clearing agents used to reduce the concentration of circulating bispecific antibody before administration of the labeled hapten should further increase the safety of AES pretargeting.

## REFERENCES

- Press OW, Eary JF, Appelbaum FR, et al. Phase II trial of I-131-B1 (anti-CD20) antibody therapy with autologous stem cell transplantation for relapsed B cell lymphomas. *Lancet* 1995;346:336–340.
- Kaminski MS, Zasadny KR, Francis IR, et al. Radioimmunotherapy of B-cell lymphoma with  $^{131}\text{I}$ -anti-B1 (anti-CD20) antibody. *N Engl J Med* 1993;329:459–465.
- Juweid M, Sharkey RM, Behr T, et al. Radioimmunotherapy of medullary thyroid cancer with iodine-131-labeled anti-CEA antibodies. *J Nucl Med* 1996;37:905–911.
- Behr TM, Sharkey RM, Juweid ME, et al. Phase I/II clinical radioimmunotherapy with an iodine-131-labeled anti-carcinoembryonic antigen murine monoclonal antibody IgG. *J Nucl Med* 1997;38:858–870.
- Rosebrough SF. Two-step immunological approaches for imaging and therapy. *Quarterly J Nucl Med* 1996;40:234–251.
- Le Doussal JM, Martin M, Gautherot E, Delaage M, Barbet J. In vitro and in vivo targeting of radiolabeled monovalent and divalent haptens with dual specificity monoclonal antibody conjugates: enhanced divalent hapten affinity for cell-bound antibody conjugate. *J Nucl Med* 1989;30:1358–1366.
- Le Doussal JM, Gruaz-Guyon A, Martin M, Gautherot E, Delaage M, Barbet J. Targeting of indium-111-labeled bivalent hapten to human melanoma mediated by bispecific monoclonal antibody conjugates: imaging of tumors hosted in nude mice. *Cancer Res* 1990;50:3445–3452.
- Manetti C, Rouvier E, Gautherot E, Loucif E, Barbet J, Le Doussal JM. Targeting BCL<sub>2</sub> lymphoma with anti-idiotypic antibodies: biodistribution kinetics of directly labeled antibodies and bispecific antibody-targeted bivalent haptens. *Int J Cancer* 1997;71:1000–1009.
- Le Doussal JM, Chetanneau A, Guyon-Gruaz A, et al. Bispecific monoclonal antibody-mediated targeting of an indium-111-labeled DTPA dimer to primary colorectal tumors: pharmacokinetics, biodistribution, scintigraphy and immune response. *J Nucl Med* 1993;34:1662–1671.
- Bardies M, Bardet S, Faivre-Chauvet A, et al. Dosimetric study using a bispecific antibody and a  $^{131}\text{I}$ -labeled bivalent hapten in patients with medullary thyroid carcinoma and small-cell lung cancer. *J Nucl Med* 1996;37:1853–1859.
- Glennie MJ, McBride HM, Worth AT, Stevenson GT. Preparation and performance of bispecific  $\text{F}(\text{ab}')_2$  antibody containing thioether-linked Fab'g fragments. *J Immunol* 1987;139:2367–2375.
- Janevik-Ivanovska E, Gautherot E, Hilairat de Boisferon M, et al. Bivalent hapten peptides designed for iodine-131 pretargeted radioimmunotherapy. *Bioconjug Chem* 1997;8:526–533.
- Covell DG, Barbet J, Holton OD, Black CD, Weinstein JN. Pharmacokinetics of monoclonal immunoglobulin G<sub>1</sub>,  $\text{F}(\text{ab}')_2$ , and Fab' in mice. *Cancer Res* 1986;46:3669–3978.
- Johns HE, Cunningham JR. The physics of radiology. In: Friedmann M, eds. *Monograph in the bannerstone division of American lectures in radiation therapy*, 3rd ed. Springfield, IL: Charles C. Thomas; 1978:564–574.
- Quadri SM, Lai J, Mohammadpour H, Vriesendorp HM, Williams JR. Assessment of radiolabeled stabilized  $\text{F}(\text{ab}')_2$  fragments of monoclonal antiferritin in nude mouse model. *J Nucl Med* 1993;34:2152–2159.
- Goodwin DA, Meares CF, David GF, et al. Monoclonal antibodies as reversible equilibrium carriers of radiopharmaceuticals. *Nucl Med Biol* 1986;13:383–391.
- Blumenthal RD, Sharkey RM, Haywood L, et al. Targeted therapy of athymic mice bearing GW-39 human colonic cancer micrometastases with  $^{131}\text{I}$ -labeled monoclonal antibodies. *Cancer Res* 1992;52:6036–6044.
- Sharkey RM, Motta-Hennessy C, Pawlyk D, Siegel JF, Goldenberg DM. Biodistribution and radiation dose estimates for yttrium-and iodine-labeled monoclonal antibody IgG and fragments in nude mice bearing human colonic tumor xenografts. *Cancer Res* 1990;50:2330–2336.
- Sung C, Van Osdol WW. Pharmacokinetic comparison of direct antibody targeting with pretargeting protocols based on streptavidin-biotin binding. *J Nucl Med* 1995;36:867–876.
- Santos O, Kindle Payne J, Domitrowsky JB, Berkeley C, Mackensen DG. A two step delivery system utilizing a bi-specific monoclonal antibody for radioimmunotherapy. *Antibody Immunoconj Radiopharm* 1995;8:93–109.
- Baxter LT, Zhu H, Mackensen DG, Butler WF, Jain RK. Biodistribution of monoclonal antibodies: scale-up from mouse to human using a physiologically based pharmacokinetic model. *Cancer Res* 1995;55:4611–4522.
- Le Doussal JM, Gautherot E, Martin M, Barbet J, Delaage M. Enhanced in vivo targeting of an asymmetric bivalent hapten to double-antigen-positive mouse B cells with monoclonal antibody conjugate cocktails. *J Immunol* 1991;146:169–175.
- Goodwin DA, Meares CF, McTigue M, et al. Pretargeted immunoscintigraphy: effect of hapten valency on murine tumor uptake. *J Nucl Med* 1992;33:2006–2013.
- Schumacher J, Klivenyi G, Matys R, et al. Multistep tumor targeting in nude mice using bispecific antibodies and a gallium chelate suitable for immunoscintigraphy with positron emission tomography. *Cancer Res* 1995;55:115–123.
- Kranenborg MH, Boerman OC, Oosterwijk-Wakka JC, De Weijert MC, Corstens FH, Oosterwijk E. Two-step radio-immunotargeting of renal cell carcinoma xenografts in nude mice with anti-renal-cell-carcinoma x anti-DTPA bispecific monoclonal antibodies. *Int J Cancer* 1998;75:74–80.
- Casalini P, Luisson E, Menard S, Colnaghi MI, Paganelli G, Canevari S. Tumor pretargeting: role of avidin/streptavidin on monoclonal antibody internalization. *J Nucl Med* 1997;38:1378–1381.
- Paganelli G, Magnani P, Zito F, et al. Three-step monoclonal antibody tumor targeting in carcinoembryonic antigen-positive patients. *Cancer Res* 1991;51:5960–5969.
- Ratliff B, Reno J, Axworthy D, et al. Performance of antibody streptavidin pretargeting in patients: initial results. *J Nucl Med* 1995;36:225P.
- Buchsbaum DJ, Langmuir VK, Wessels BW. Experimental radioimmunotherapy. *Med Phys* 1993;20:551–567.
- Devys A, Thedrez P, Gautherot E, et al. Comparative targeting of human colon-carcinoma multicell spheroids using one- and two-step (bispecific antibody) techniques. *Int J Cancer* 1996;67:883–891.
- Thames HD, Hendry JH. Radiation-induced injury to tissues. In: Thames HD, ed. *Fractionation in radiotherapy*. London: Taylor and Francis; 1987:1–21.
- Sgouras G. Bone marrow dosimetry for radioimmunotherapy: theoretical considerations. *J Nucl Med* 1993;34:689–694.
- Manetti C, Le Doussal JM, Rouvier E, Gruaz-Guyon A, Barbet J. Intracellular uptake and catabolism of anti-IgM antibodies and bi-specific antibody-targeted hapten by B-lymphoma cells. *Int J Cancer* 1995;63:250–256.
- West GB, Brown JH, Enquist BJ. A general model for the origin of allometric scaling laws in biology. *Science* 1997;276:122–126.